Correlating carrier lifetime with device design and photovoltaic performance of perovskite solar cells

View Online   Export Citation   CrossMark

Shiqiang Fu,[1] Jiahao Wang,[1] Like Huang,[1,a] (iD) Xiaohui Liu,[1] (iD) Jing Zhang,[1] (iD) Ziyang Hu,[1] (iD) and Yuejin Zhu[1,2,a] (iD)

AFFILIATIONS

[1]Department of Microelectronic Science and Engineering, School of Physical Science and Technology, Ningbo Collaborative Innovation Center of Nonlinear Calamity System of Ocean and Atmosphere, Ningbo University, Ningbo 315211, China
[2]School of Information Engineering, College of Science and Technology, Ningbo University, Ningbo 315300, China

[a]Authors to whom correspondence should be addressed: huanglike@nbu.edu.cn and zhuyuejin@nbu.edu.cn

ABSTRACT

Efficient electron transport layer-free perovskite solar cells (ETL-free PSCs) are promising designs because they offer low-cost, simpler device configuration and greatly promote the large area flexible application of PSCs. Meanwhile, compared to traditional PSCs with ETL, the development of ETL-free PSCs is hindered by their low performance due to serious interfacial energy loss. Herein, we reveal that ETL-free devices with relatively low carrier lifetimes of perovskite films exhibit more substantial photogenerated carrier loss, resulting in a lower electron-injection rate at the FTO (fluorine-containing tin oxide)/perovskite interface, which is mainly responsible for the performance loss. Moreover, we demonstrate that improving the carrier lifetimes of perovskite films can remedy the poor carrier extraction efficiency at the FTO/perovskite interface through three typical perovskite films. Similarly, for all-inorganic perovskite with lower carrier lifetime and hole transport layer-free devices, prolonging carrier lifetime may be an important measure to improve the device performance. Benefiting from this discovery, increasing the carrier lifetime of the perovskite films can counterbalance the inferior device interfaces, endowing the ETL-free PSCs with high performance close to that of the ETL devices. Our research provides insights into ETL-free PSCs and offers opportunities for high-performance ETL-free PSC device design.

Published under an exclusive license by AIP Publishing. https://doi.org/10.1063/5.0070632

As a promising photovoltaic technology, perovskite solar cells (PSCs) have drawn worldwide interest from both academic and industrial community. The power conversion efficiency (PCE) of PSCs has grown from 3.8% to 25.5% over the past decade, gradually surpassing the state-of-the-art performance of conventional crystalline silicon solar cells.[1–6] So far, most PSCs with high efficiencies are based on the traditional mesoporous n-i-p device configurations in which distinct n-type electron transport layer (ETL) and p-type hole transport layer (HTL) are generally recognized as critical components for effective separation and extraction of photogenerated carriers.[7] The extensively utilized and efficient ETL materials reported in studies are the inorganic n-type TiO_2 and SnO_2 compact layers.[8–10] However, the TiO_2 ETL based PSCs usually suffer from severe hysteresis and TiO_2/perovskite interface instability due to oxygen vacancies induced ultraviolet photocatalytic degradation and proton reaction of perovskite.[10–15] Moreover, the PSCs with solution-processed ETL, such as SnO_2 and ZnO, face the same problems of hysteresis and instability.[10,16] Moreover, these ETL-induced

issues lead to prospects of the complex production process, high cost, and difficulties in constructing more all-purpose perovskite optoelectronics.[17] Accordingly, researchers have made many efforts to remove the carrier transport layer to construct ETL-free PSCs. In fact, the excellent ambipolar charge transport characteristics of perovskite materials endow great potential to construct PSCs with a simplified device architecture.[18–21] In our previous work, we have systematically studied the effects of perovskite material engineering, energy band engineering, and interface engineering on the performance of ETL-free PSCs.[22–27] More importantly, many studies have shown that perovskite has superior performance in carrier dissociation and transport, and transparent electrodes (such as fluorine-containing tin oxide, FTO) themselves are typical n-type semiconductors.[18,19,28] Therefore, for perovskite films with long carrier lifetimes, theoretically it is possible to achieve excellent photovoltaic performance without ETL.

In this work, we investigate the device performance of $CsPbI_2Br$, $MAPbI_3$, and $FA_{0.9}Cs_{0.1}PbI_{3-x}Cl_x$ with different carrier lifetimes in the

ETL-free and ETL devices to correlate their carrier lifetimes with different device design and photovoltaic performance of PSCs, so as to find a clue to further improve the device performance of ETL-free PSCs through carrier dynamics engineering. As a result, we reveal that ETL-free PSCs with relatively low carrier lifetimes of perovskite films exhibit more substantial photogenerated carrier energy loss compared with ETL based devices. In other words, the perovskite composition with longer carrier lifetime has improved tolerance to surface defects and non-radiative recombination. Moreover, the contact layer is mostly affecting the fill factor (FF) of the different carrier lifetimes PSCs, which decreases considerably when using only FTO contact, while open circuit voltage (Voc) and short circuit current (Jsc) remain very similar. Also, we have demonstrated that improving carrier lifetimes of the perovskite film can enhance the carrier collection

efficiency at the FTO/perovskite interface, making the carrier dynamics in ETL-free devices essentially as good as those high-performance ETL based PSCs. Benefiting from this discovery, our research provides an insight into the ETL-free PSCs. Accordingly, higher performance ETL-free PSCs with a simple device design can be obtained through carrier dynamics engineering in future.

To identify the difference in photovoltaic performance between typical ETL-free and ETL PSCs, we fabricated ETL-free and ETL devices with the device architectures of glass/FTO/($CsPbI_2Br$, $MAPbI_3$, $FA_{0.9}Cs_{0.1}PbI_{3-x}Cl_x$)/spiro-MeOTAD/Ag and glass/FTO/SnO_2/($CsPbI_2Br$, $MAPbI_3$, $FA_{0.9}Cs_{0.1}PbI_{3-x}Cl_x$)/spiro-MeOTAD/Ag, respectively. Figures 1(a)–1(c) show the J-V curves of the best-performing ETL-free and ETL PSCs based on $CsPbI_2Br$, $MAPbI_3$, and $FA_{0.9}Cs_{0.1}PbI_{3-x}Cl_x$ perovskite, respectively. The corresponding
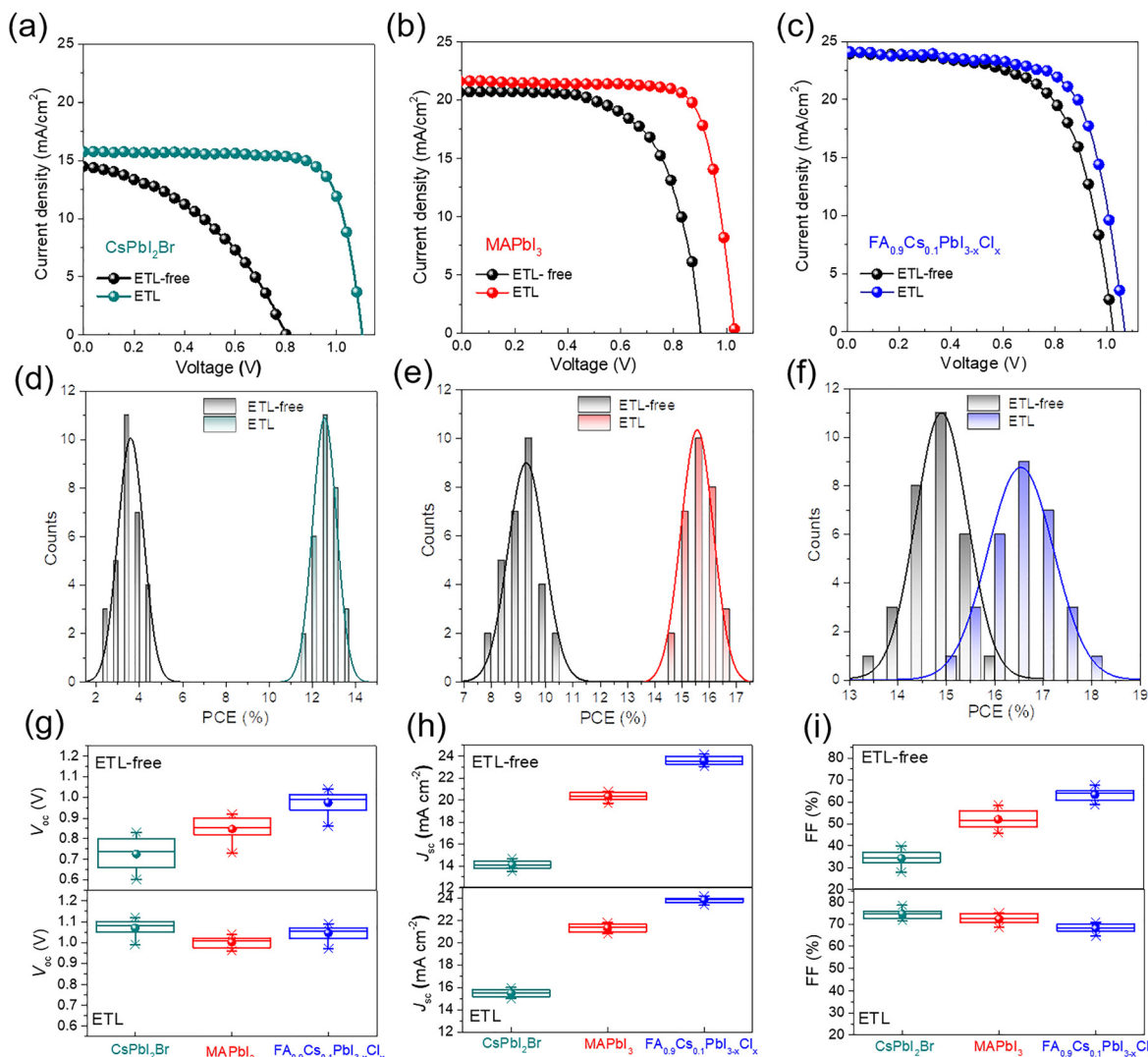

FIG. 1. J-V curves of the best-performing ETL-free and ETL PSCs prepared with a (a) $CsPbI_2Br$, (b) $MAPbI_3$, and (c) $FA_{0.9}Cs_{0.1}PbI_{3-x}Cl_x$ film. PCE distributions for ETL-free and ETL PSCs prepared with a (d) $CsPbI_2Br$, (e) $MAPbI_3$, and (f) $FA_{0.9}Cs_{0.1}PbI_{3-x}Cl_x$ film. Photovoltaic parameters statistics for 30 independent ETL-free and ETL PSC devices with $CsPbI_2Br$, $MAPbI_3$, and $FA_{0.9}Cs_{0.1}PbI_{3-x}Cl_x$: (g) V_{OC}, (h) J_{SC}, and (i) FF.

TABLE I. Photovoltaic parameters of various devices.

Device	Voc (V)	Jsc (mA/cm^2)	Fill factor (%)	Efficiency (%)
CsPbI$_2$Br (ETL-free)	0.82	14.49	36.58	4.34
CsPbI$_2$Br (ETL)	1.10	15.75	78.46	13.59
MAPbI$_3$ (ETL-free)	0.91	20.65	55.96	10.51
MAPbI$_3$ (ETL)	1.03	21.59	74.12	16.48
FA$_{0.9}$Cs$_{0.1}$PbI$_{3-x}$Cl$_x$ (ETL-free)	1.03	23.95	64.91	16.01
FA$_{0.9}$Cs$_{0.1}$PbI$_{3-x}$Cl$_x$ (ETL)	1.07	24.01	70.56	18.13

photovoltaic parameters are shown in Table I. As a result, the PCE of CsPbI$_2$Br and MAPbI$_3$ based ETL-free devices is 4.34% and 10.51%. With ETL, the CsPbI$_2$Br and MAPbI$_3$ devices have a PCE of 13.59% and 16.48%. It is clear that for CsPbI$_2$Br and MAPbI$_3$, the PCE of the ETL-free device is significantly lower than that of a typical ETL based device, and this phenomenon is most obvious in CsPbI$_2$Br devices. Nevertheless, for FA$_{0.9}$Cs$_{0.1}$PbI$_{3-x}$Cl$_x$ devices, the device efficiency (16.01%) of the ETL-free device is close to that (18.13%) of the ETL based device. For the above results, we can infer that the ETL is indispensable mostly for the CsPbI$_2$Br perovskite, following with MAPbI$_3$ perovskite, to obtain high-performance PSCs, while for FA$_{0.9}$Cs$_{0.1}$PbI$_{3-x}$Cl$_x$, ETL is not necessary for high-performance PSCs.

For the sake of further study of the performance differences of different perovskites based ETL-free and ETL devices, we conducted further statistical analysis on 30 devices under optimal conditions. Figures 1(d)–1(f), respectively, present the PCE statistical results of CsPbI$_2$Br, MAPbI$_3$, and FA$_{0.9}$Cs$_{0.1}$PbI$_{3-x}$Cl$_x$ devices with ETL-free and ETL based structures. The average PCE of the ETL-free and ETL CsPbI$_2$Br PSC is 3.1% and 12.6%, respectively. Obviously, ETL has a great impact on the device performance of CsPbI$_2$Br based PSCs. With MAPbI$_3$ as an absorb layer, the average PCE of the ETL-free and ETL device becomes closer to each other, which are 9.8% and 15.1%, respectively. Interestingly, there is a small difference between the average PCE of the FA$_{0.9}$Cs$_{0.1}$PbI$_{3-x}$Cl$_x$ based ETL-free and ETL devices, which are 15.4% and 16.8%, respectively. From the PCEs of the six ETL-free and ETL devices with three different perovskites, we can reach the conclusion that the ETL is an indispensable part of the high-performance devices with CsPbI$_2$Br and MAPbI$_3$ perovskites, but for the ETL-free of FA$_{0.9}$Cs$_{0.1}$PbI$_{3-x}$Cl$_x$ perovskite, the high-performance devices can also be obtained. This implies that certain intrinsic parameters of different perovskite absorb layers determine the different degree influence of ETL on the device performance and, thus, determine the design of an efficient device structure. The identification of this intrinsic parameter will be of great significance for device design, and it is expected to obtain efficient and simple PSCs through effective regulation of this intrinsic parameter.

In order to find and determine this parameter, more experimental results are needed. Figures 1(g)–1(i) are statistical box plots of Voc, Jsc, and FF of three perovskites of CsPbI$_2$Br, MAPbI$_3$, and FA$_{0.9}$Cs$_{0.1}$PbI$_{3-x}$Cl$_x$ with ETL-free and ETL structures. It can be observed that the trend of Voc, Jsc, and FF is similar to the trend of PCE, illustrating that for CsPbI$_2$Br and MAPbI$_3$ perovskites, the ETL is indispensable for high-performance devices, but for the FA$_{0.9}$Cs$_{0.1}$PbI$_{3-x}$Cl$_x$ perovskite, the ETL is negligible. As the FF of a PSC device depends heavily on the defect concentration and carrier

lifetime of the perovskite adopted, we, thus, speculate that the carrier lifetime of different perovskites may be the key factor affecting the performance of different device structures. Moreover, previous studies have shown that for a given perovskite, improved carrier lifetime can indeed enhance the device performance, making the carrier dynamics in the ETL-free device essentially as good as those in the ETL device.[29] This is consistent with our above conjecture that the different effect of ETL on the performance of different perovskite devices is mainly due to the different carrier lifetime.

Therefore, we have measured the carrier lifetime of the three perovskite materials. Figures 2(a)–2(c) are the time-resolved photoluminescence (TRPL) measurements of CsPbI$_2$Br, MAPbI$_3$, and FA$_{0.9}$Cs$_{0.1}$PbI$_{3-x}$Cl$_x$ films on quartz substrates, respectively. By fitting the PL decay curve with a biexponential function as below, we can get the carrier lifetime:[30,31]

$$F(t) = A_1 \exp(-t/\tau_1) + A_2 \exp(-t/\tau_2), \qquad (1)$$

where the short-lifetime τ_1 presents the surface recombination, the long-lifetime τ_2 corresponds to the bulk recombination, and A$_1$ and A$_2$ are the respective amplitudes. As a result, τ_1 and τ_2 of the CsPbI$_2$Br film are 0.52 and 4.03 ns, respectively. The MAPbI$_3$ film exhibits longer lifetimes of 3.52 ns for τ_1 and 20.80 ns for τ_2, compared with the CsPbI$_2$Br film. However, compared to the CsPbI$_2$Br and MAPbI$_3$ films, τ_1 and τ_2 of the FA$_{0.9}$Cs$_{0.1}$PbI$_{3-x}$Cl$_x$ film are significantly improved to 9.07 and 77.01 ns. Similarly, the average carrier lifetimes (τ_{avg}) of CsPbI$_2$Br, MAPbI$_3$, and FA$_{0.9}$Cs$_{0.1}$PbI$_{3-x}$Cl$_x$ also show the same trend, which are 3.95, 19.68, and 74.94 ns, respectively. To further confirm the accuracy of τ_{avg}, we present the statistical results of the τ_{avg} of three perovskites (Table S1). In addition, from the TRPL (Figure S1) results of three different perovskite films on the substrate FTO or SnO$_2$, we can infer that the ETL is indispensable mostly for the CsPbI$_2$Br perovskite, following with MAPbI$_3$ perovskite, to obtain high carrier extraction efficiency, while for FA$_{0.9}$Cs$_{0.1}$PbI$_{3-x}$Cl$_x$, ETL is not necessary for high carrier extraction efficiency. From Figs. 2(d), 2(e), and 2(f), τ_1, τ_2, and τ_{avg} of three perovskites of CsPbI$_2$Br, MAPbI$_3$, and FA$_{0.9}$Cs$_{0.1}$PbI$_{3-x}$Cl$_x$ show the same trend of change, although significantly difference in the τ_{avg} of the CsPbI$_2$Br, MAPbI$_3$, and FA$_{0.9}$Cs$_{0.1}$PbI$_{3-x}$Cl$_x$ films from several nanoseconds to several ten nanoseconds can be observed. More importantly, the trend of carrier lifetimes is similar to that of device parameters, illustrating that close correlation between the device performances and the carrier lifetimes of perovskite adopted and that long carrier lifetimes substantially benefit the ETL-free device performance. Therefore, the obvious difference in the τ_{avg} of the above three types of perovskite films indicates that the carrier lifetime may be an important factor affecting the performance of the ETL-free device.
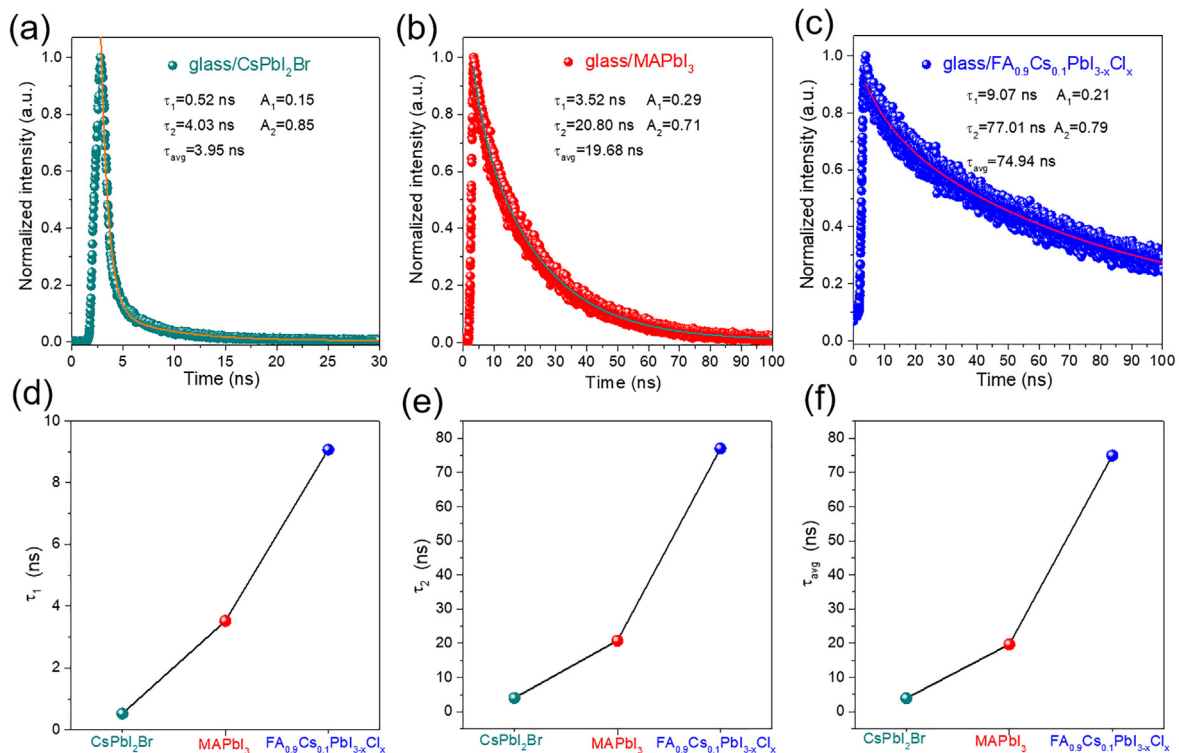
FIG. 2. TRPL spectra of (a) $CsPbI_2Br$, (b) $MAPbI_3$, and (c) $FA_{0.9}Cs_{0.1}PbI_{3-x}Cl_x$ film. $CsPbI_2Br$, $MAPbI_3$, and $FA_{0.9}Cs_{0.1}PbI_{3-x}Cl_x$ perovskite films of (d) τ_1, (e) τ_2, and (f) τ_{avg}.

Considering that the carrier lifetime is related to the crystallinity and defect state of the film, large crystal grains generally have a longer carrier lifetime.[32] Therefore, we conducted surface scanning electron microscopy (SEM) tests on the three types of perovskite films. Generally, different substrates with varying surface properties and roughness may have certain effects on the growth and optoelectronics properties of perovskite films.[33] In order to exclude the serious influence of different substrates on the structure, morphology and optoelectronic properties of perovskite films, we deposited $CsPbI_2Br$, $MAPbI_3$, and $FA_{0.9}Cs_{0.1}PbI_{3-x}Cl_x$ films on glass/FTO and glass/FTO/SnO_2 substrates, respectively. The SEM patterns of the corresponding films with glass/FTO substrate are presented in Figs. 3(a)–3(c). The SEM patterns of the $CsPbI_2Br$, $MAPbI_3$, and $FA_{0.9}Cs_{0.1}PbI_{3-x}Cl_x$ films on the glass/FTO/SnO_2 substrate are presented in Figs. 3(d)–3(f). (Cross section is shown in Fig. S2.) From this result, we can deduce that the $CsPbI_2Br$, $MAPbI_3$, and $FA_{0.9}Cs_{0.1}PbI_{3-x}Cl_x$ films share similar film grain size, morphologies, and compactness on both substrates. In addition, the optical absorption spectra (Fig. S3) illustrate that the $CsPbI_2Br$, $MAPbI_3$, and $FA_{0.9}Cs_{0.1}PbI_{3-x}Cl_x$ films also have similar optical features with almost coincident curves on both substrates. These results indicate that glass/FTO and glass/FTO/SnO_2 substrates have little effect on the basic structural and optoelectronics properties of perovskite films. Since the glass/FTO and glass/FTO/SnO_2 substrates have nearly the same optical absorption features and the perovskite films have similar grain structures, the reduced PCE in ETL-free devices likely derives from the different interfaces. We analyzed the band energy positions of three different perovskite materials at the interface of FTO or SnO_2 (Fig. S4). Due to the difference in WF of FTO or SnO_2 and perovskite, Schottky barrier associated with spontaneous band bending can be formed when these two materials contact. As a result, it can be found that the FTO interface is extremely advantageous for the collection of $CsPbI_2Br$ (downward band bending) perovskite carriers, but it is unfavorable for $MAPbI_3$ and $FA_{0.9}Cs_{0.1}PbI_{3-x}Cl_x$ (upward band bending) perovskites. In addition, the SnO_2 interface shows that although the effect of ETL on the energy level arrangement of $CsPbI_2Br$ and $FA_{0.9}Cs_{0.1}PbI_{3-x}Cl_x$ is similar, the performance improvement in the two perovskite devices is significantly different. This is probably due to the difference in the carrier lifetime of the perovskite, which leads to a huge difference in the sensitivity to ETL. For $CsPbI_2Br$ with a shorter carrier lifetime, ETL is necessary to improve the device performance, while for $FA_{0.9}Cs_{0.1}PbI_{3-x}Cl_x$ with a longer carrier lifetime, ETL has negligible impact on improving device performance. In short, ETL does help to reduce the electron barrier and block holes, which is beneficial for improving the performance of the device. However, for perovskites with long carrier lifetimes, even if the energy levels at the interface are not matched, excellent device performance can still be obtained. Only for those perovskites with low carrier lifetimes, ETL is particularly important for improving the device performance. More importantly, Fig. S5 shows that ETL-free devices also have excellent stability, similar to the stability of ETL devices. This shows that ETL-free devices have great development potential for the commercialization of PSCs in the future.
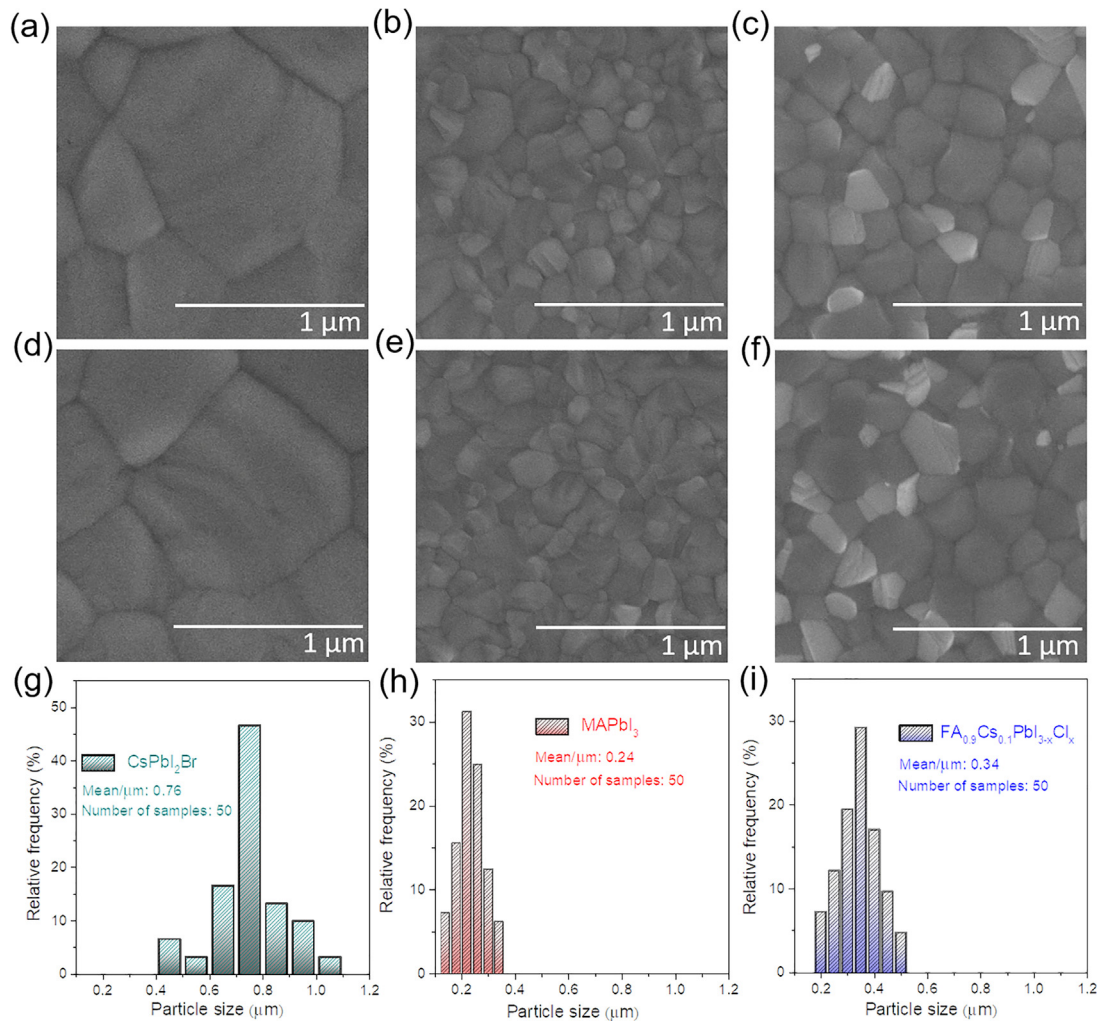
FIG. 3. Top-view SEM images of (a) $CsPbI_2Br$, (b) $MAPbI_3$, and (c) $FA_{0.9}Cs_{0.1}PbI_{3-x}Cl_x$ films with the glass/FTO substrate. Top-view SEM images of (d) $CsPbI_2Br$, (e) $MAPbI_3$, and (f) $FA_{0.9}Cs_{0.1}PbI_{3-x}Cl_x$ films with the glass/FTO/SnO_2 substrate. Statistical distribution based on the calculated grain sizes of (g) $CsPbI_2Br$, (h) $MAPbI_3$, and (i) $FA_{0.9}Cs_{0.1}PbI_{3-x}Cl_x$ films with the glass/FTO/SnO_2 substrate from their corresponding SEM images.

Generally, crystal defects ($N_{t\text{-total}}$) are composed of the following three parts:

$$N_{t\text{-total}} = N_{t\text{-GI}} + N_{t\text{-GB}} + N_{t\text{-surface}}, \tag{2}$$

where $N_{t\text{-GI}}$ is the grain interior defects, $N_{t\text{-GB}}$ is the grain boundary defects, and $N_{t\text{-surface}}$ is the grain surface defects. It is well established that the prolonged carrier lifetime is strongly related to the reduction in defect density at grain interior and boundary as well as surface.[34,35] We speculate that the grain size of $CsPbI_2Br$, $MAPbI_3$, and $FA_{0.9}Cs_{0.1}PbI_{3-x}Cl_x$ films increases in sequence, which leads to the reduction in grain boundary defects, thereby prolonging the carrier lifetime. Figures 3(g)–3(i) are the statistical distribution diagrams of the grain sizes of $CsPbI_2Br$, $MAPbI_3$, and $FA_{0.9}Cs_{0.1}PbI_{3-x}Cl_x$ films, respectively. There is no change in the grain size statistics of $CsPbI_2Br$, $MAPbI_3$, and $FA_{0.9}Cs_{0.1}PbI_{3-x}Cl_x$ films with ETL-free (Fig. S6) and the grain size statistics of ETL. Interestingly, however,

the average grain size of the $CsPbI_2Br$ ($0.76\,\mu m$) film with the shortest carrier lifetime is much larger than that of the $FA_{0.9}Cs_{0.1}PbI_{3-x}Cl_x$ ($0.34\,\mu m$) film with the longest carrier lifetime. Usually, larger crystal grains have longer carrier lifetime.[37] Taking the stereotyped ETL/perovskite/HTL structure as an example, there are at least five carrier recombination pathways in the bulk perovskite layer and related interfaces (Fig. S7). The results of space charge limited current (SCLC) and urbach energy (Fig. S8) indicate that the grain boundary defects of the $CsPbI_2Br$ film have a subordinate effect on the carrier lifetime, while the grain interior and the grain surface defect primarily affect the device performance. Also, for the same type of all-inorganic perovskite, the $N_{t\text{-GI}}$ is considered the same, and the $N_{t\text{-surface}}$ may be an important reason for the lower carrier lifetime. This is consistent with extensive reports that the interface defect passivation significantly improves the performance of all-inorganic perovskite solar cell devices.

From the above discussion, the device performance is closely related to the carrier lifetime. To explore the degree to which the carrier lifetimes can impact the ETL-free and ETL PSCs, respectively, we display the correlations between $FA_{0.9}Cs_{0.1}PbI_{3-x}Cl_x$ carrier lifetime of $CsPbI_2Br$, $MAPbI_3$, and $FA_{0.9}Cs_{0.1}PbI_{3-x}Cl_x$ and the device parameters. From Fig. 4(a), it is found that the PCE of ETL-free (black line) devices is substantially more sensitive to the carrier lifetimes than ETL (purple line) devices. Figure 4(b) gives the relationship between the carrier lifetime (purple line) of the perovskite film and the PCE value (black line) difference (Δ_{PCE}) between ETL-free and ETL based PSCs. Obviously, with the increase in the carrier lifetime of the different perovskite film, Δ_{PCE} decreases rapidly, indicating that increasing the carrier lifetimes of perovskite films may boost the PCE of associated ETL-free perovskite solar cells to the same level as ETL PSCs. Figure 4c shows the trend of FF change values (Δ_{FF}) with the carrier lifetime, similar to Δ_{PCE}, and Δ_{FF} decreases rapidly as the carrier lifetime increases, which also indicates that extending the carrier lifetime favors the performance of the ETL-free device. In addition, from the results of stabilized power output (SPO) PCEs (Fig. S9), it can be found that three different perovskites based ETL-free and ETL devices display a steady PCE under the same operation, indicating that it also has an excellent operational stability for the ETL-free based devices. The results of Figs. S9 and S11 show that increasing the carrier life is conducive to reducing the hysteresis (the values of HI are shown in Tables S2 and S3) and increasing the recombination resistance (R_{rec}) of the device.

Previous seminal works have shown that the ETL has a huge impact on Voc, which is attributed to the reduction of built-in potential.[36] Interestingly, with ETL, the Voc of all the three different

perovskite based PSC devices of $FA_{0.9}Cs_{0.1}PbI_{3-x}Cl_x$ is close to 1 V [Fig. 4(d)]. In Fig. 4(e), the small change value of Voc (Δ_{Voc}) in the device with ETL-free and ETL indicates that the difference in the contact layer has little influence on Voc. In addition, Jsc [Fig. 1(h)] of $CsPbI_2Br$, $MAPbI_3$, and $FA_{0.9}Cs_{0.1}PbI_{3-x}Cl_x$ also has similar behaviors and hardly change with the cell configuration. To verify the electronic structure of the different contact layers, we analyzed them by ultraviolet photoelectron spectroscopy (UPS). The results are presented in Fig. S10, and the extracted work functions are also illustrated in Fig. 4(f), in comparison with Voc. As expected, the FTO layer has a higher work function of 4.75 eV, followed by SnO_2 (4.15 eV). Obviously, there is no distinct relationship between the Voc of the device and the work function of the contact layer, as the qVoc difference in ETL-free and ETL based devices (0.04–0.28 eV) is much smaller than the work function difference (0.6 eV). We speculate that the difference in carrier lifetime weakens the influence of the work function of the contact layer, and it will be more obvious for devices with longer carrier lifetime (such as $FA_{0.9}Cs_{0.1}PbI_{3-x}Cl_x$), making the Voc (1.04 V) of ETL-free close to the Voc of ETL (1.07 V). Therefore, improving the carrier lifetime of the perovskite film can reduce the influence of the contact layer on photovoltaic parameters, enabling the device performance in ETL-free to approach that in ETL devices.

To better understand the difference in the device performance, steady-state photoluminescence (PL) measurements were carried out to study the interfacial effects induced by FTO and FTO/SnO_2. Figures 5(a)–5(c) are the PL of $CsPbI_2Br$, $MAPbI_3$, and $FA_{0.9}Cs_{0.1}PbI_{3-x}Cl_x$, respectively. Obviously, the FTO/SnO_2 (blue line) substrate exhibited more efficient PL quenching of the perovskite layer than that based on single-layer FTO (red line), indicating a stronger
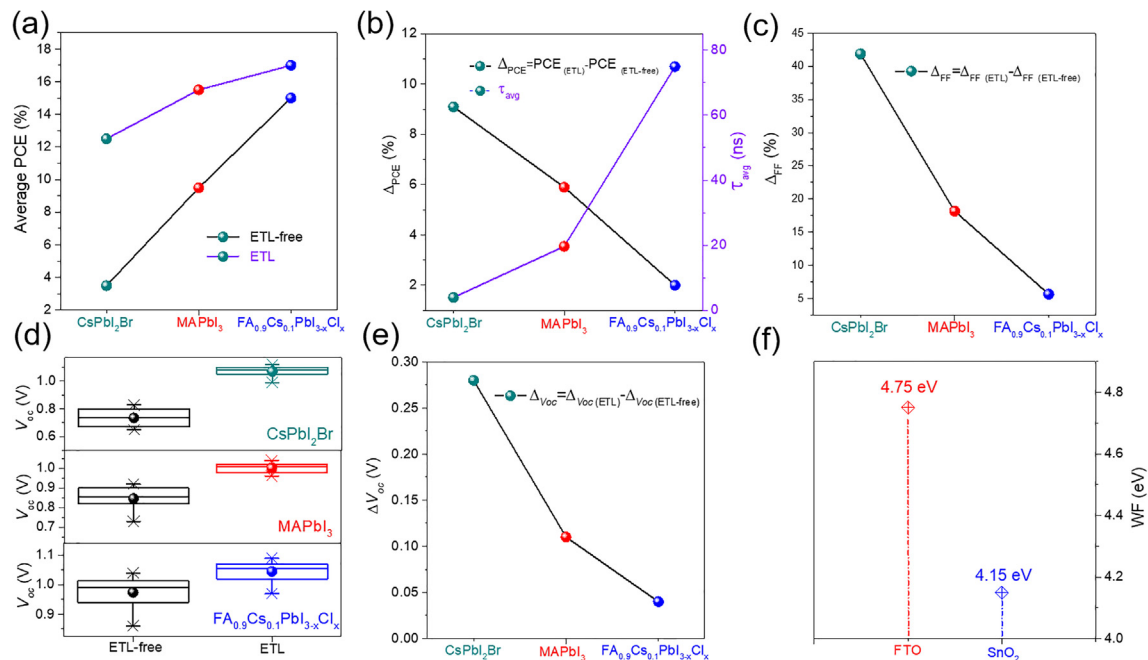

FIG. 4. (a) The average PCE values of ETL-free and ETL PSCs based on $CsPbI_2Br$, $MAPbI_3$, and $FA_{0.9}Cs_{0.1}PbI_{3-x}Cl_x$. (b) The correlations between τ_{avg} of $CsPbI_2Br$, $MAPbI_3$, and $FA_{0.9}Cs_{0.1}PbI_{3-x}Cl_x$ films and Δ_{PCE} for ETL-free and ETL PSCs. (c) The Δ_{FF} for ETL-free and ETL PSCs. (d) Voc distributions for ETL-free and ETL PSCs prepared with $CsPbI_2Br$, $MAPbI_3$, and $FA_{0.9}Cs_{0.1}PbI_{3-x}Cl_x$ films. (e) The Δ_{Voc} for ETL-free and ETL PSCs. (f) The work function of the FTO and SnO_2.
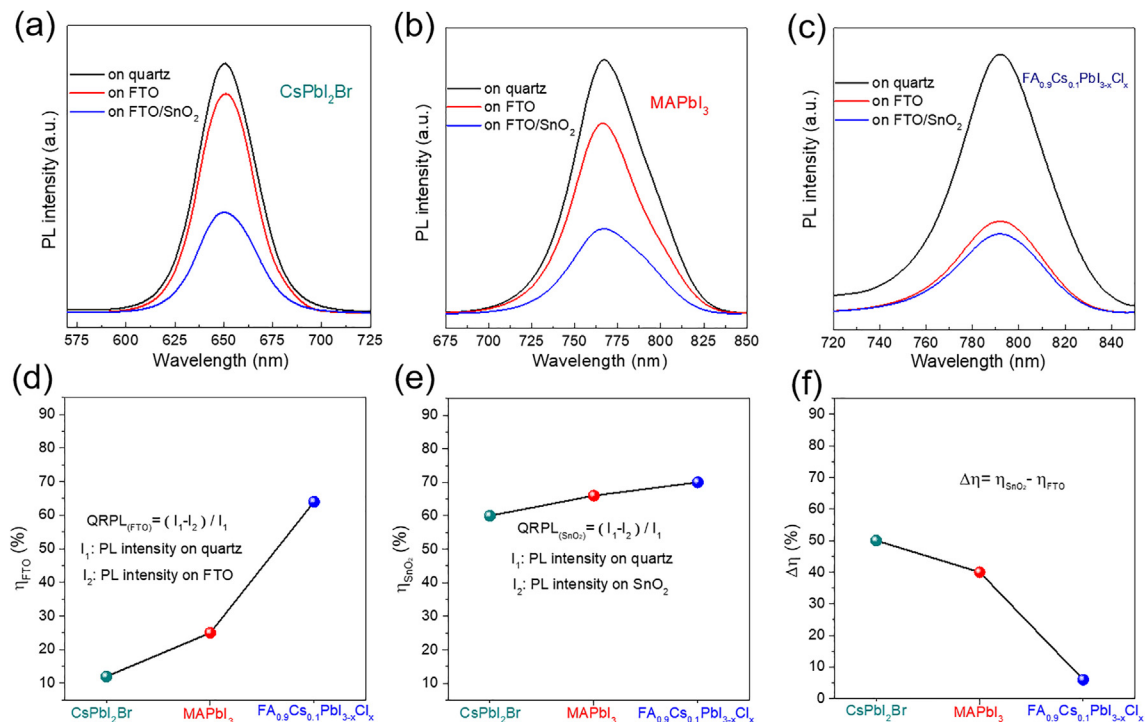
FIG. 5. The steady-state PL spectra of (a) $CsPbI_2Br$, (b) $MAPbI_3$, and (c) $FA_{0.9}Cs_{0.1}PbI_{3-x}Cl_x$ films on quartz, glass/FTO, and glass/FTO/SnO$_2$ substrates, respectively. (d) The η_{FTO} of the $CsPbI_2Br$, $MAPbI_3$, and $FA_{0.9}Cs_{0.1}PbI_{3-x}Cl_x$ films. (e) The η_{SnO2} of the $CsPbI_2Br$, $MAPbI_3$, and $FA_{0.9}Cs_{0.1}PbI_{3-x}Cl_x$ films. (f) The $\Delta\eta$ of the $CsPbI_2Br$, $MAPbI_3$, and $FA_{0.9}Cs_{0.1}PbI_{3-x}Cl_x$ films.

electron extraction capability from the different perovskite films. Furthermore, perovskite films are differently sensitive to ETL due to the carrier lifetime. For $CsPbI_2Br$ with short carrier lifetime, the extraction electron of the ETL interface is particularly important, but for long carrier lifetime perovskite films, the extraction electron of the ETL-free interface is comparable to ETL, which is most obvious in the $FA_{0.9}Cs_{0.1}PbI_{3-x}Cl_x$ film.

To further investigate the influence of ETL on the carrier collection efficiency, we define a PL quenching rate metric (QR$_{PL}$), QR$_{PL}$ = $(I_1-I_2)/I_1$, where I_1 is the PL intensity of the perovskite film on quartz while I_2 is the value on FTO or FTO/SnO$_2$, which is better to evaluate the carrier injection. For Fig. 5(d) with ETL-free, as the carrier lifetime increases, the electron extraction efficiency is significantly improved, indicating that a longer carrier lifetime is essential for improving the extraction efficiency of electrons with ETL-free. For Fig. 5(e), which contains the ETL, the extraction efficiency slowly rises with the prolongation of the same carrier lifetime, indicating that the effect of the ETL on electron extraction is far less than the longer carrier lifetime. In order to better illustrate the influence of ETL-free and ETL on the electron injection rate of the perovskite interface with different carrier lifetimes, we calculated the change values ($\Delta\eta$) of η_{SnO2} and η_{FTO}, as shown in Fig. 5(f). As a result, for $CsPbI_2Br$ with a short carrier lifetime, the ETL has a great influence on the extraction efficiency of electrons. Nevertheless, for $FA_{0.9}Cs_{0.1}PbI_{3-x}Cl_x$ with a longer carrier lifetime, the extraction efficiency of ETL for electrons is negligible. Therefore, with the increase in the carrier lifetime, the influence of

the ETL on the interface extraction efficiency decreases, which is consistent with the changing trend of the previous device performance parameters with the carrier lifetime. From the above results, we can draw the following conclusions. The ETL is not the only and key factor that affects the extraction efficiency of electrons at the interface. Only when the carrier lifetime is small and the value is fixed or does not change much, the effect of ETL on the extraction of electrons becomes prominent. For those perovskite films with long carrier lifetimes, the electron extraction efficiency of ETL-free can also be comparable to that with ETL.

In summary, we used three perovskites with significantly different carrier lifetimes as the absorption layers to compare and analyze the effect of ETL on the device performance. The results show that for the same type of perovskite, the ETL indeed affects the device performance to different extent, but our work shows that when the perovskite film is optimized to increase the carrier lifetime, the impact of ETL on the device performance decreases significantly. Therefore, compared with ETL, the carrier lifetime of the perovskite film has a greater impact on the device performance. More importantly, if the carrier lifetime of the perovskite material is substantially enhanced (such as microsecond carrier lifetimes), the device structure can be appropriately simplified without necessarily adopting the complex n-i-p structure. Therefore, a longer carrier life is important for simple and efficient ETL-free devices. Furthermore, it is necessary to find effective methods to improve the carrier life, thereby boosting the performance of devices. Our work suggests that for simple devices with no hole

transport layer, higher carrier lifetime may also be the key to improving the device performance. In addition, our results also show that the all-inorganic perovskite has a larger grain size and a lower grain boundary defect density than the organic–inorganic hybrid perovskite, but its carrier lifetime is far less than the latter, suggesting that for all-inorganic perovskite, surface defects could be the important factors leading to the lower carrier lifetime. This is consistent with extensive reports that the interface defect passivation significantly improves the performance of all-inorganic PSC devices. In short, our work has established the relationship between carrier lifetime and device design and device performance, which will help to design other efficient and simplified perovskite solar cells in the future to promote the realization of low-cost perovskite solar cell applications.

See the supplementary material for the experimental section, summary table (τ_{avg}) of the reported $CsPbI_2Br$, $MAPbI_3$, and $FA_{0.9}Cs_{0.1}PbI_{3-x}Cl_x$ films, UV-vis absorption, device stability and hysteresis, SPO, UPS, and Figs. S1–S11.

AUTHOR DECLARATIONS

Conflict of Interest

The authors have no conflicts to disclose.

Author Contributions

The manuscript was written through contributions of all authors. All authors have given approval to the final version of the manuscript.

DATA AVAILABILITY

The data that support the findings of this study are available within this article and its supplementary material.

REFERENCES

[1]A. Kojima, K. Teshima, Y. Shirai, and T. Miyasaka, J. Am. Chem. Soc. **131**, 6050 (2009).

[2]H. S. Kim, C. R. Lee, J. H. Im, K. B. Lee, T. Moehl, A. Marchioro, S. J. Moon, R. Humphry-Baker, J. H. Yum, J. E. Moser, M. Gratzel, and N. G. Park, Sci. Rep. **2**, 591 (2012).

[3]H. Lu, Y. Liu, P. Ahlawat, A. Mishra, W. R. Tress, F. T. Eickemeyer, Y. Yang, F. Fu, Z. Wang, C. E. Avalos, B. I. Carlsen, A. Agarwalla, X. Zhang, X. Li, Y. Zhan, S. M. Zakeeruddin, L. Emsley, U. Rothlisberger, L. Zheng, A. Hagfeldt, and M. Gratzel, Science **370**, eabb8985 (2020).

[4]M. Jeong, I. W. Choi, E. M. Go, Y. Cho, M. Kim, B. Lee, S. Jeong, Y. Jo, H. W. Choi, J. Lee, J.-H. Bae, S. K. Kwak, D. S. Kim, and C. Yang, Science **369**, 1615 (2020).

[5]G. Kim, H. Min, K. S. Lee, D. Y. Lee, S. M. Yoon, and S. I. Seok, Science **370**, 108 (2020).

[6]See https://www.nrel.gov/pv/assets/pdfs/best-research-cell-efficiencies.20200929.pdf for "Solar efficiency chart," National Renewable Energy Laboratory, 2020.

[7]J. Shi, X. Xu, D. Li, and Q. Meng, Small **11**, 2472 (2015).

[8]J. A. Christians, P. Schulz, J. S. Tinkham, T. H. Schloemer, S. P. Harvey, B. J. Tremolet de Villers, A. Sellinger, J. J. Berry, and J. M. Luther, Nat. Energy **3**, 68 (2018).

[9]W. Li, W. Zhang, S. Van Reenen, R. J. Sutton, J. Fan, A. A. Haghighirad, M. B. Johnston, L. Wang, and H. J. Snaith, Energy Environ. Sci. **9**, 490 (2016).

[10]T. Leijtens, G. E. Eperon, S. Pathak, A. Abate, M. M. Lee, and H. J. Snaith, Nat. Commun. **4**, 2885 (2013).

[11]H. J. Snaith, A. Abate, J. M. Ball, G. E. Eperon, T. Leijtens, N. K. Noel, S. D. Stranks, J. T. Wang, K. Wojciechowski, and W. Zhang, J. Phys. Chem. Lett. **5**, 1511 (2014).

[12]L. Huang, J. Xu, X. Sun, C. Li, R. Xu, Y. Du, J. Ni, H. Cai, J. Li, Z. Hu, and J. Zhang, J. Alloy Compd. **735**, 224 (2018).

[13]S. K. Pathak, A. Abate, P. Ruckdeschel, B. Roose, K. C. Gödel, Y. Vaynzof, A. Santhala, S.-I. Watanabe, D. J. Hollman, N. Noel, A. Sepe, U. Wiesner, R. Friend, H. J. Snaith, and U. Steiner, Adv. Funct. Mater. **24**, 6046 (2014).

[14]J. Yang, B. D. Siempelkamp, E. Mosconi, F. De Angelis, and T. L. Kelly, Chem. Mater. **27**, 4229 (2015).

[15]Y. Cheng, Q. D. Yang, J. Xiao, Q. Xue, H. W. Li, Z. Guan, H. L. Yip, and S. W. Tsang, ACS. Appl. Mater. Interfaces **36**, 19986 (2015).

[16]B. Chen, M. Yang, S. Priya, and K. Zhu, J. Phys. Chem. Lett. **7**, 905 (2016).

[17]Z. Li, Y. Zhao, X. Wang, Y. Sun, Z. Zhao, Y. Li, H. Zhou, and Q. Chen, Joule **2**, 1559 (2018).

[18]G. Xing, N. Mathews, S. Sun, S. S. Lim, Y. M. Lam, M. Grätzel, S. Mhaisalkar, and T. C. Sum, Science **342**, 344–347 (2013).

[19]S. D. Stranks, G. E. Eperon, G. Grancini, C. Menelaou, M. J. P. Alcocer, T. Leijtens, L. M. Herz, A. Petrozza, and H. J. Snaith, Science **342**, 341 (2013).

[20]L. Huang and Z. Ge, Adv. Energy Mater. **24**, 1900248 (2019).

[21]L. Huang, J. Wang, and Y. Zhu, J. Phys. Chem. Lett. **12**, 2266 (2021).

[22]L. Huang, Z. Hu, J. Xu, X. Sun, Y. Du, J. Ni, H. Cai, J. Li, and J. Zhang, Sol. Energy Mater. Sol. Cell **149**, 1 (2016).

[23]L. Huang and Y. Zhu, Appl. Phys. Lett. **5**, 0034441 (2021).

[24]L. Huang, S. Bu, D. Zhang, R. Peng, Q. Wei, Z. Ge, and J. Zhang, Sol. RRL. **2**, 1800274 (2019).

[25]L. Huang, D. Zhang, S. Bu, R. Peng, Q. Wei, and Z. Ge, Adv. Sci. **7**, 1902656 (2020).

[26]L. Huang, J. Xu, X. Sun, Y. Du, H. Cai, J. Ni, J. Li, Z. Hu, and J. Zhang, ACS. Appl. Mater. Interfaces **8**, 9811 (2016).

[27]L. Huang and Y. Zhu, Adv. Electron. Mater. **7**, 2100006 (2021).

[28]V. D'Innocenzo, G. Grancini, M. J. P. Alcocer, A. R. S. Kandada, S. D. Stranks, M. M. Lee, G. Lanzani, H. J. Snaith, and A. Petrozza, Nat. Commun. **1**, 3586 (2014).

[29]Q. Han, J. Ding, Y. Bai, T. Li, J.-Y. Ma, Y.-X. Chen, Y. Zhou, J. Liu, Q.-Q. Ge, J. Chen, J. T. Glass, M. J. Therien, J. Liu, D. B. Mitzi, and J.-S. Hu, Chem **4**, 2405 (2018).

[30]W. Chen, H. Chen, G. Xu, R. Xue, S. Wang, Y. Li, and Y. Li, Joule **3**, 191 (2019).

[31]S. Fu, X. Li, L. Wan, Y. Wu, W. Zhang, Y. Wang, Q. Bao, and J. Fang, Adv. Energy Mater. **35**, 1901852 (2019).

[32]H. Fan, F. Li, P. Wang, Z. Gu, J. H. Huang, K. J. Jiang, B. Guan, L. M. Yang, X. Zhou, and Y. Song, Nat. Commun. **1**, 5402 (2020).

[33]J. Ma, J. Su, Z. Lin, L. Zhou, J. He, J. Zhang, S. Liu, J. Chang, and Y. Hao, Nano Energy **67**, 104241 (2020).

[34]W. Liu, N. Liu, S. Ji, H. Hua, Y. Ma, R. Hu, J. Zhang, L. Chu, X. Li, and W. Huang, Nano-Micro Lett. **12**, 119 (2020).

[35]A. Fathi, E. Jokar, Y. P. Lee, and E. W. Diau, Angew. Chem. Int. Ed. **43**, 19001 (2020).

[36]N. J. Jeon, J. H. Noh, W. S. Yang, Y. C. Kim, S. Ryu, J. Seo, and S. I. Seok, Nature **517**, 476 (2015).

[37]M.-R. Sui, S.-P. Li, and X.-Q. Gu, Optoelectron. Lett. **15**, 117 (2019).